Korean J. Chem. Eng., **27**(1), 289-298 (2010)
DOI: 10.1007/s11814-009-0350-0

An empirical near-critical correction for a quasi-chemical nonrandom lattice fluid

Ju Ho Lee*, Gap Su Han*, Alexander Breitholz*, Ki-Pung Yoo*, Moon Sam Shin, and Hwayong Kim***,†**

*Department of Chemical and Biomolecular Engineering, Sogang University,
Sinsu-dong, Mapo-gu, Seoul 121-742, Korea
**Department of Cosmetic Science, Chungwoon University,
San 29, Namjang-ri, Hongseong-eup, Hongseong-gun, Chungnam 350-701, Korea
***School of Chemical & Biological Engineering, Seoul National University,
San 56-1, Shilim-dong, Gwanak-gu, Seoul 151-744, Korea
(*Received 2 September 2009 • accepted 27 September 2009*)

Abstract−This paper proposes a simple empirical correction to improve the near-critical volumetric behavior of a classical equation of state (EOS) which overpredicts the critical point. The focus is on the alternative representation of long-range density fluctuation, an effect neglected in classical EOS, in terms of molecular clustering. To formulate the molecular clustering of interest, the Veytsman statistics is extended and fluctuation parameter is explicitly obtained as a solution to the quadratic equation. The proposed contribution was combined with a quasi-chemical nonrandom lattice fluid (QLF), which overpredicts the critical point. The combined model was found to require three clustering parameters besides three classical parameters and tested against vapor-liquid equilibrium data consisting of 43 nonpolar and polar components. The calculation results showed that the combined model satisfactorily represents the flattened part of the critical isotherm curve for methane as well as the top of the coexistence curve for the tested components.

Key words: Veytsman Statistics, Long-range Density Fluctuation, Molecular Clustering, Critical Region, Probability Function

INTRODUCTION

Advances in chemical and industrial engineering require thermodynamic models capable of describing various properties over wide ranges of temperature and pressure. When applied in normal conditions far from the critical point, classical equations of state (EOS) [1-3] can accurately calculate and predict physical properties. However, such equations of state often fail to satisfactorily reproduce physical properties near the critical region where thermodynamic properties show a singular behavior [4]. The reason lies in that classical EOS are based on mean field approximation which neglects long-range density fluctuation near the critical point [5].

Several strategies [6-10] have been proposed to overcome the deficiency of classical EOS in describing physical properties near the critical point. These strategies can be classified as empirically or theoretically based. The empirical approach divides the Helmholtz energy contribution into classical and fluctuating contribution. Based on this approach, some analytic fluctuation terms [6-8] were developed, tested against light components and found to improve volumetric behavior near the critical point. However, these approaches [6,7] were mainly applicable to equations of state which match critical point (T_c, P_c and V_c) and thus not applicable to equations of state which overpredict the critical point, such as SAFT and Lattice fluid theory. The theoretical approach considers long-range density fluctuation and formulates it by statistical mechanics. Renormalization group theory [10] and crossover theory [9] are good examples of the theoretical-based approach. The former is based on phase-space cell approximation [11,12] as well as the Hamiltonian in White's work [13,14], and the latter is founded on classical Landau expansion [15] around the critical point. These approaches, extended to diverse frameworks such as cubic [9,16], hard-sphere [17,18] and lattice fluid [19], accurately represent thermodynamic properties over a wide range of temperature and pressure. However, they possess some disadvantages as well. Renormalization group theory requires numerical integration, indicating that EOS cannot be explicitly expressed. In crossover theory, several parameters are required to fit experimental data due to its phenomenology, and the significance of long-range density fluctuation has not been clarified [20].

The purpose of this study is to develop an empirical correction for EOS which overpredicts the critical point. To derive a correction, we attempt to alternatively model long-range density fluctuation effect in terms of molecular clustering. Molecular clustering, which is generally found between molecules forming hydrogen bonds as well as polar fluids, is modeled by well-known thermodynamic models such as chemical theory [21], Wertheim's theory [22,23] and Veytsman statistics [24]. However research [25,26] has shown that even non-hydrogen bonding molecules can form clusters (or aggregates) near the critical region. Pfund and co-workers [25] showed by small angle x-ray scattering (SAXS) that the number of xenon aggregates increases near the critical density. Tucker and Maddox [27] showed by molecular simulation that clustering between particles occurs around a critical point.

In phase equilibria, the concept of molecular clustering near the critical region was first introduced by Heideman and Prausnitz [21].

†To whom correspondence should be addressed.
E-mail: Hwayongk@snu.ac.kr
‡This paper is dedicated to Professor Jae Chun Hyun for celebrating his retirement from Department of Chemical and Biological Engineering of Korea University.

They showed that the introduction of clustering effect by chemical theory leads to an improved critical isotherm for argon. However, for non-hydrogen bonding molecules, this approach was not extended to the calculation of other physical properties such as saturated vapor pressure, saturated liquid density, and supercritical isotherm data. Moreover, the application of hydrogen bonding theory to this type of clustering requires standard hydrogen bonding theory to be flexible enough to describe a clustering dominant near the critical density, since such theories were originally developed to account for clustering in high-density regions. In this work, Veytsman statistics is applied because it provides a probability function adjusting the region where clustering is dominant. Lee et al. [28] concluded in their work that Veytsman statistics is flexible enough to account for other types of clustering such as intra-molecular hydrogen bonds. We modify its probability function to be maximized near the critical density.

The derived near-critical correction is combined with basic QLF EOS [29], a lattice-based EOS which shows a comparable result with SAFT for pure and mixtures but overpredicts a critical point. In section 2, we discuss the qualitative effects of molecular clustering on pressure-density isotherms near the critical region. The formulation of molecular clustering with modified Veytsman statistics is described in section 3. Data for saturated vapor pressure, saturated liquid density, critical point and supercritical pressure-density are presented in section 4.

EFFECT OF MOLECULAR CLUSTERING ON PRESSURE-DENSITY ISOTHERM

Classical EOS are based on mean field approximation theory, which neglects the contribution of density fluctuation to free energy density. For pure fluid, this theory [30] assumes the immediate environment of each molecule has the same density as the bulk fluid, which is therefore regarded as homogeneous. However, as the system approaches the critical point, density fluctuations across the long-range become correlated and considerably alter the free energy density. These fluctuations lead to system nonhomogeneeity and molecules forms clusters somewhat different from the stable and strong clusters formed by hydrogen bonds [26,27]. We present the effect of long-range density fluctuation on the systems in Fig. 1 where each box represents the systems under different conditions. In the framework of mean field approximation (Fig. 1(a)), no molecules become clustered as the system is considered as homogeneous (upper central box). However, in the presence of long-range density fluctuation (Fig. 1(b)), the molecules in the critical region are clustered and aggregation occurs (lower central box).

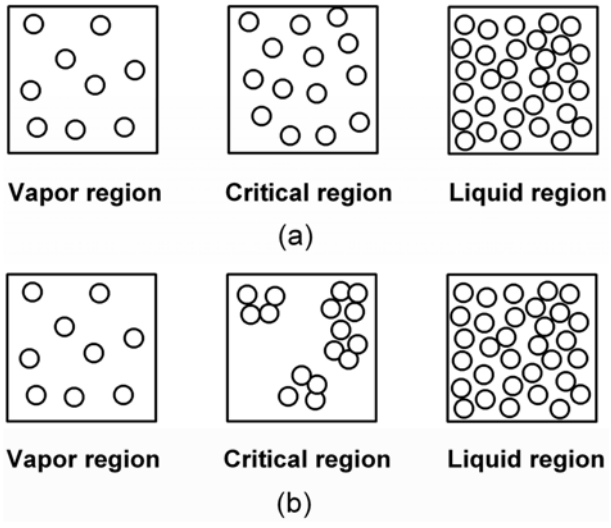

Fig. 1. Distribution of molecules in the systems without (upper boxes) and with long-range density fluctuation (lower boxes).

Before proceeding with model development, some further discussion is appropriate. We assume that the Helmholtz energy is divided into both classical and long-range density fluctuation contribution and molecular clustering shares behavior similar to that of long-range density fluctuation. Let us denote Ω_{cla} as a classical configurational partition function. If we assign Ω_{mc} as a partition function solely accounting for molecular clustering effect, the correct total configuration partition function, Ω_{tot}, can be factorized as

$$\Omega_{tot}=\Omega_{cla}\Omega_{mc}. \tag{1}$$

The Ω_{mc} has two boundary conditions. As it is associated with the number of ways to distribute clustered molecules, it has a value of 1 at regions far from critical point and reaches some maximum value near the critical region. Fig. 2(a) is a schematic showing the behavior of Ω_{cla}.

The pressure can be derived from a partition function by the following relation,

$$P=-kT\rho_m^2\left(\frac{\partial \ln \Omega}{\partial \rho_m}\right)_T \tag{2}$$

where k is Boltzmann constant and ρ_m is molar density. We denote P_{cla} and P_{mc} as pressures corresponding to Ω_{cla} and Ω_{mc}, respectively, which are related by the following equation,

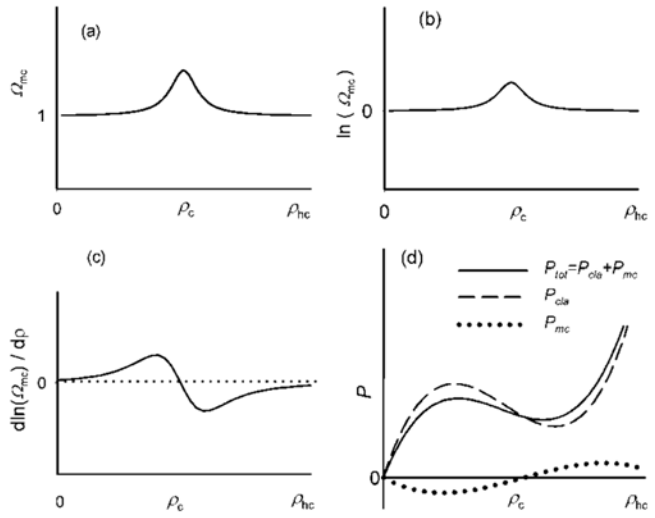

Fig. 2. Schematics of density dependence of clustering effect to density: (a) Ω_{mc} (b) ln(Ω_{mc}) (c) a derivative of Ω_{mc} with respect to density (d) Effect of Ω_{mc} on P-ρ isotherm: P_{cla}, isotherm by classical EOS; P_{mc}, isotherm by clustering effect; P_{tot}, isotherm by classical EOS incorporating clustering effect.

$$P_{tot} = -kT\rho_m^2\left(\frac{\partial \ln \Omega_{cla}}{\partial \rho_m}\right)_T - kT\rho_m^2\left(\frac{\partial \ln \Omega_{mc}}{\partial \rho_m}\right)_T = P_{cla} + P_{mc} \quad (3)$$

Eq. (3) reveals the effect of clustering on P-ρ isotherm. Suppose that the system is approaching critical temperature and clustering is likewise most dominant near critical density, ρ_c. This indicates that Ω_{mc} is maximized at ρ_c (Fig. 2(a)). Logarithmic Ω_{mc}, $\ln(\Omega_{mc})$, displays similar behavior with Ω_{mc}, nearly always constant far from critical point and convex at ρ_c (Fig. 2(b)) Therefore, its derivative with respect to density displays a positive convex shape between 0 and ρ_c and a negative concave shape between ρ_c and ρ_{hc}, which stands for hard-core density (Fig. 2(c)). From the viewpoint of pressure, the molecular clustering contribution makes a negative correction at densities lower than ρ_c, while a positive pressure correction is made at densities higher than ρ_c. Fig. 2(d) shows the molecular clustering effect leads to flattened P_{tot} (solid line) compared with P_{cla} (long-dashed line).

To exactly reproduce the critical point, P_{cla} should satisfy following constraint,

$$P_{cla}(T_c, \rho_c) = P_c \quad (4)$$

because P_{mc} should be zero at ρ_c (Fig. 2(d)). However, we found that well-known classical EOS do not obey the above constraint. Fig. 3 shows the isotherms of ethane calculated by SAFT (solid line) and Sanchez-Lacombe EOS (small-dashed line) at the critical temperature. Filled triangle and empty triangle represent the calculated pressure of SAFT and the Sanchez-Lacombe EOS, respectively, at the experimental critical density. It is clear both models underestimate the pressure when compared with the experimental critical pressure (filled box). This implies P_{tot} is unable to exactly reproduce a critical pressure if molecular clustering is maximized at the experimental critical density. Chou et al. [6] found a similar problem in applying their fluctuation term to SRK EOS and attempted to resolve it by employing a volume translation method. But, as their approach yields a discontinuous P-ρ isotherm, we solve this problem in a different way. We observe that the densities of the two models (filled circle and empty circle) of which the pressure reproduces P_c are located left of ρ_c. Thus, our basic assumption is modified as follows: The density where molecular clustering reaches maximum is shifted left of the experimental critical density.

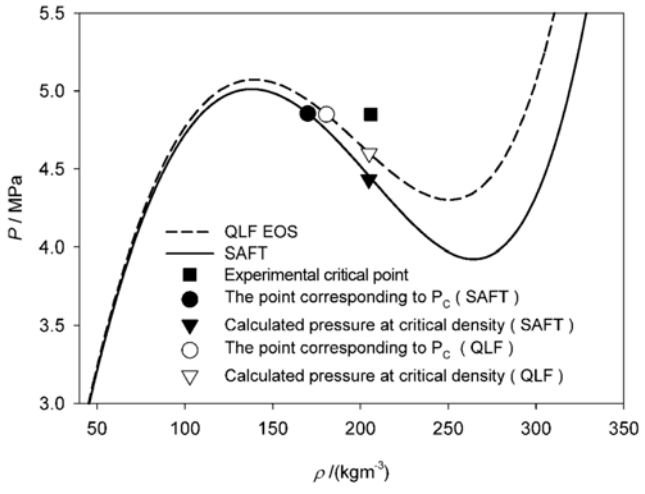

Fig. 3. The P-ρ isotherms of ethane with predictions of SAFT [3] and QLF EOS [29] at T=305.32 K.

EXTENDED VEYTSMAN STATISTICS

Veytsman statistics [24] was proposed to account for the n-mer cluster due to hydrogen bond. However, before extending Veytsman statistics to the present molecular clustering, we briefly discuss their basic formulation. In pure hydrogen bonding components with a single type of donor and acceptor, the number of ways of distributing N_{HB}, the number of hydrogen bonding pairs between donor and acceptor, among N_1 molecules is,

$$\Xi_0 = \frac{(N_1 a)!(N_1 d)!}{(N_1 a - N_{HB})!(N_1 d - N_{HB})!}\frac{1}{N_{HB}} \quad (5)$$

where a and d are the number of donors and acceptors per molecule, respectively. Eq. (5) assumes that donors and acceptors of hydrogen bonding pairs are not necessarily adjacent to each other. Furthermore, as hydrogen bonding occurs between nearby donors and acceptors, the exact number of ways of distributing N_{HB} pairs between the donor and acceptor is defined as,

$$\Xi = \Xi_0 p_{HB} \quad (6)$$

where p_{HB} is the probability that the donor and acceptor are located in close proximity and hydrogen bonding occurs. Panayiotou and Sanchez [31] proposed p_{HB} as,

$$p_{HB} = \frac{1}{N_r} e^{\frac{S_{HB}}{k}} = \frac{\rho}{rN_1} e^{\frac{S_{HB}}{k}} \quad (7)$$

where N_r is total number of lattice sites composed of N_0 holes and N_1 r-mers, r is segment length of the pure component, ρ is the reduced density or volume fraction defined as rN_1/N_r and S_{HB} is entropy change resulting from hydrogen bond formation. Eq. (7) indicates the contribution of hydrogen bonding is negligible at low densities and significant at high densities. The canonical partition function for the contribution of hydrogen bonding is,

$$\Omega_{HB} = \Xi e^{-\beta E_{HB} N_{HB}} = \left(\frac{\rho}{rN_1}\right)^{N_{HB}} \frac{(N_1 a)!(N_1 d)!}{(N_1 a - N_{HB})!(N_1 d - N_{HB})!}\frac{1}{N_{HB}!} e^{-\beta(E_{HB} - TS_{HB})N_{HB}} \quad (8)$$

where E_{HB} is hydrogen bonding energy. The last exponential term on the right represents the dependence of hydrogen bonding on temperature.

As clustering due to long-range density fluctuation is assumed to be negligible in the region far from the critical point, the probability for such clustering is empirically proposed as

$$p_{mc} = \frac{\rho^m}{rN_1}(1-\rho)^n e^{\frac{S_{mc}}{k}} \quad (9)$$

where S_{mc} is entropy change due to cluster formation and the exponents m and n represent the rate of rise and fall of p_{mc} in low and high density regions, respectively. All these values are positive. The proposed probability function satisfies the following boundary condition: it becomes negligible at low and high density regions because ρ and $1-\rho$ lead the Eq. (9) to zero as $\rho \to 0$ and 1, respectively. Eq. (7) is maximum at the density $\rho^* = m/(n+m)$.

To derive a partition function for molecular clustering near the

Table. 1. Pure component parameters in the present model for 43 components

Substance	M/gmol^{-1}	V_H	r	ε	m	n	$10^{-3}\chi$	T range	AARD (%)		Ref.	
									P^{sat}	ρ^{sat}	P^{sat}	ρ^{sat}
Gases												
Carbon dioxide	44.010	4.40	6.98	70.13	4.01	10.95	0.936	216.55-303.00	1.02	0.17	[38]	[38]
Carbon monoxide	28.010	5.98	5.34	32.70	3.95	9.65	0.332	68.14-129.85	1.30	0.78	[38]	[38]
Argon	39.948	6.14	4.44	39.49	3.91	8.96	0.209	83.78-150.00	0.64	0.93	[38]	[38]
Nitrogen	28.014	6.35	4.98	31.91	3.73	9.10	0.213	63.15-126.00	1.12	0.91	[38]	[38]
Oxygen	31.999	5.31	4.92	39.21	3.60	8.72	0.170	61.00-154.00	2.64	1.81	[38]	[38]
Sulfur dioxide	70.905	7.66	5.56	102.74	3.52	8.98	0.226	183.15-416.48	3.10	1.78	[38]	[38]
Alkanes												
Methane	16.043	7.92	4.51	50.12	3.31	7.82	0.095	91.00-190.53	1.47	1.32	[39]	[39]
Ethane	30.070	8.74	5.71	74.83	3.05	8.14	0.119	129.00-305.25	3.58	1.43	[40]	[40]
Propane	44.097	10.01	6.64	86.18	4.04	10.86	0.855	167.00-369.00	2.91	1.14	[40]	[40,41]
n-Butane	58.123	11.24	7.37	96.21	4.14	11.67	1.327	191.00-425.00	2.50	1.05	[40]	[40,41]
n-Pentane	72.150	12.33	8.05	103.96	4.13	11.97	1.735	217.00-468.00	1.93	1.20	[40]	[40,41]
n-Hexane	86.177	13.30	8.71	110.23	3.93	11.98	1.543	244.00-507.00	1.93	1.31	[40]	[40,41]
n-Heptane	100.204	14.13	9.37	115.43	3.81	12.06	1.619	264.00-540.00	2.19	1.30	[40]	[40,41]
n-Octane	114.231	14.58	10.16	119.08	3.63	12.11	1.507	288.00-568.00	1.94	1.79	[40]	[40,41]
n-Nonane	128.258	15.54	10.72	123.13	3.45	12.14	1.363	320.00-580.00	1.85	1.05	[33]	[33]
n-Decane	142.285	15.88	11.40	126.32	3.36	11.90	1.285	340.00-600.00	1.56	2.11	[33]	[33]
Branchedalkanes												
2-Methylpropane	58.123	11.81	7.13	93.12	3.47	10.09	0.366	187.00-408.00	3.11	1.19	[40]	[40,41]
2-Methylbutane	72.150	12.92	7.70	102.87	3.02	9.44	0.250	213.00-447.00	1.84	1.63	[40]	[40]
2,3-Dimethylbutane	86.177	14.77	7.83	111.50	3.32	10.19	0.412	259.00-499.00	1.49	1.53	[40]	[40,41]
2-Methylpentane	86.177	14.02	8.30	109.51	3.24	10.24	0.420	236.00-497.00	2.70	1.26	[40]	[40,41]
Cycloalkanes												
Cyclopentane	70.134	11.42	7.38	115.43	2.97	9.40	0.187	229.00-510.00	2.68	1.64	[40]	[40,41]
Cyclohexane	84.161	13.45	7.47	124.63	3.60	10.62	0.571	279.00-547.00	1.78	1.12	[40]	[40,41]
Methylcyclopentane	84.161	13.33	7.69	119.37	3.65	10.76	0.663	256.00-532.00	1.87	1.19	[40]	[40,41]
Methylcyclohexane	98.188	15.32	7.76	127.98	3.36	10.27	0.422	276.00-572.00	2.25	1.19	[40]	[40,41]
Ethylcyclopentane	98.188	15.01	8.03	126.59	3.28	10.16	0.420	293.00-569.00	2.23	0.80	[40,41]	[40,41]
Alkenes												
Ethylene	28.054	8.04	5.63	69.18	3.84	9.68	0.385	120.00-282.30	3.06	1.01	[42]	[42]
Propylene	42.081	9.29	6.58	85.01	4.41	11.58	1.430	157.00-364.00	2.67	1.18	[40]	[40]
1-Butene	56.108	10.92	7.14	95.77	4.29	11.76	1.549	195.00-418.00	1.72	0.98	[40,41]	[40,41]
1-Pentene	70.134	12.07	7.81	103.67	4.00	11.58	1.277	215.00-463.00	2.28	0.97	[40]	[40,41]
1-Hexene	84.161	12.95	8.61	109.14	3.76	11.60	1.145	283.00-493.00	0.80	0.53	[40,41]	[40,41]
1-Octene	112.215	14.37	9.92	119.27	3.67	12.04	1.582	287.00-558.00	1.13	2.38	[40,41]	[40,41]
Benzene derivative												
Benzene	78.114	11.31	7.38	127.53	3.71	10.62	0.647	278.00-562.00	2.19	0.74	[40]	[40,41]
Toluene	92.141	11.83	8.45	129.00	3.28	10.32	0.492	273.00-584.00	2.32	1.53	[40]	[40,41]
Styrene	104.152	12.56	8.79	138.06	3.04	9.77	0.383	301.00-630.00	2.91	1.42	[40,41]	[40,41]
m-Xylene	106.167	13.32	8.75	134.96	2.99	9.57	0.339	302.00-616.00	2.31	1.09	[40]	[40,41]
o-Xylene	106.167	13.17	8.73	137.26	2.94	9.61	0.280	303.00-630.00	1.92	1.27	[40]	[40,41]
p-Xylene	106.167	13.24	8.87	133.90	2.93	9.63	0.298	296.00-616.00	1.54	0.94	[40]	[40,41]
Ketones												
Acetone	58.08	8.52	8.01	115.82	2.41	7.71	0.134	253.00-508.00	2.44	1.13	[40]	[40,41]
Methylethylketone	72.11	9.47	8.83	117.11	3.31	10.26	0.647	272.00-529.00	1.03	0.80	[40]	[40,41]
2-Pentanone	86.13	10.56	9.34	120.24	2.94	9.89	0.405	282.00-544.00	1.22	0.94	[40]	[40,41]
3-Pentanone	86.13	10.49	9.37	120.01	2.83	9.39	0.286	285.00-558.00	2.02	1.31	[40,41]	[40,41]
Etc.												
Ethylacetate	88.11	9.08	9.66	111.32	3.30	10.89	0.734	253.15-523.15	2.41	1.20	[40]	[40,41]
Dimethylether	46.07	7.95	7.00	92.50	2.75	8.26	0.120	179.45-399.66	2.83	1.07	[41,43,44]	[41,45,46]

critical region, we made the following assumption: all molecules have one donor-like and one acceptor-like site that enable multiple cluster formation. Thus, the partition function is given as

$$\Omega_{mc}=\left(\frac{\rho^m(1-\rho)^n\chi}{rN_1}\right)^{N_{mc}}\frac{(N_1)!(N_1)!}{(N_1-N_{mc})!(N_1-N_{mc})!N_{mc}!}\frac{1}{} \tag{10}$$

where $\chi=e^{-\beta(E_{mc}-TS_{mc})}$ and N_{mc} is the number of clustered molecules due to long-range fluctuation. Eq. (10) is maximized with respect to N_{mc} to give the following constraint:

$$N_{mc}N_r=(N_1-N_{mc})^2\rho^{m-1}(1-\rho)^n\chi \tag{11}$$

The Helmholtz energy of the clustering effect is given as

$$\beta A_{mc}=-\ln\Omega_{mc} \tag{12}$$

where β is the reciprocal temperature defined as 1/kT.

In a hydrogen bonding framework, χ shows a decreasing behavior as temperature increases since internal energy for hydrogen bonding formation is negative. However, this behavior cannot describe the temperature dependence of long-range density effect, vanishing away from the critical point. Thus we tested several temperature-dependent forms of χ satisfying such behavior but found that temperature independent χ can satisfactorily improve the volumetric behavior near the critical point [8].

Contributions to pressure and reduced configurational, chemical potential due to molecular clustering are represented as

$$P_{mc}=-\frac{1}{V_H\beta}\frac{N_{mc}}{N_1}\frac{\rho}{r}\left(m-n\frac{\rho}{1-\rho}\right) \tag{13}$$

$$\frac{\mu_{mc}^{conf}}{kT}=\frac{N_{mc}}{N_1}+2\ln\left(1-\frac{N_{mc}}{N_1}\right) \tag{14}$$

where V_H is the specific cell volume of the lattice. The N_{mc}/N_1 is the positive root of the Eq. (12) given as

$$\frac{N_{mc}}{N_1}=\frac{2\Delta+1-\sqrt{1+4\Delta}}{2\Delta} \tag{15}$$

where $\Delta=\rho^m(1-\rho)^n/r\chi$

The proposed contribution of molecular clustering is derived from the framework of the lattice fluid. In the present study, we apply this proposed contribution to the QLF EOS. The basic QLF EOS [29] has the form

$$P_{QLF}=\frac{1}{V_H\beta}\left[\frac{z}{2}\ln\left[1+\rho\left(\frac{q}{r}-1\right)\right]-\ln(1-\rho)-\frac{z\beta}{2}\varepsilon\theta_1^2\left(1-\frac{\beta\varepsilon}{2}\theta_0(2\theta_1-\theta_0)\right)\right] \tag{16}$$

$$\frac{\mu_{QLF}^{conf}}{RT}=r\ln\left[1+\left(\frac{q}{r}-1\right)\rho\right]-r\ln(1-\rho)+\ln\left(\frac{\theta_1}{q}\right)+\frac{z\beta}{2}\varepsilon q\left[2\theta_1-\theta_1^2+\frac{\beta\varepsilon\theta_0\theta_1}{2}(2\theta_1-\theta_0)\right] \tag{17}$$

where ε is molecular interaction energy and subscript QLF is the abbreviation of QLF EOS, and superscript conf stands for configurational property. The overall equations of the contribution pressure and chemical contribution are

Table 2. Relative deviations of correlated critical points

Substance	AARDT[c] (%)[a]	AARDP[c] (%)[a]	AARDV[c] (%)[a]
Gases			
Carbon dioxide	−0.04	0.00	0.00
Carbon monoxide	0.54	0.00	0.00
Argon	0.24	0.00	0.00
Nitrogen	0.10	−1.36	0.00
Oxygen	0.38	−0.72	0.00
Sulfur dioxide	0.00	−1.62	0.00
Alkanes			
methane	−0.02	−0.40	0.00
Ethane	−0.02	−0.61	0.00
propane	0.15	−0.99	0.00
Butane	0.00	−1.70	0.00
pentane	0.14	0.00	0.00
hexane	−0.01	0.00	0.00
heptane	0.00	−0.12	0.00
Octane	0.08	−0.81	0.00
nonane	−0.05	0.00	0.24
decane	0.00	0.00	2.92
Branched alkanes			
2-Methylpropane	−0.01	−2.81	0.00
2-Methylbutane	0.67	0.00	0.00
2,3-Dimethylbutane	0.16	−0.76	0.00
2-Methylpentane	0.01	−1.12	0.00
Cycloalkanes			
Cyclopentane	0.22	−3.96	0.00
Cyclohexane	0.29	0.00	0.00
Methylcyclopentane	0.12	−0.48	0.00
Methylcyclohexane	−0.01	−1.87	0.00
Ethylcyclopentane	0.00	0.00	0.00
Alkenes			
Ethylene	−0.03	−0.08	0.00
Propylene	0.30	0.00	0.00
1-Butene	0.12	−0.02	0.00
1-Pentene	0.12	0.00	0.00
1-Hexene	0.60	0.00	0.01
1-Octene	0.30	−0.09	0.06
Benzene derivative			
Benzene	−0.01	−1.82	0.00
Toluene	0.79	0.00	0.00
Styrene	0.71	−0.01	0.01
m-Xylene	0.09	0.00	0.00
o-Xylene	0.00	−1.77	0.00
p-Xylene	−0.01	−2.70	0.00
Ketones			
Acetone	−0.01	−1.39	0.01
Methylethylketone	0.20	0.00	0.00
2-Pentanone	0.62	−0.03	2.93
3-Pentanone	0.44	−0.51	0.01
Etc.			
Ethylacetate	0.03	−1.19	0.00
Dimethylether	0.05	−2.27	0.00
Total	0.18	0.73	0.14

[a]$AARDX=1/100(1-X^{cal}/X^{exp})$

$$P = P_{QLF} + P_{mc} = \frac{1}{V_H\beta}\left[\frac{z}{2}\ln\left[1+\rho\left(\frac{q}{r}-1\right)\right] - \ln(1-\rho) - \frac{z\beta}{2}\varepsilon\theta_1^2\left(1-\frac{\beta\varepsilon}{2}\theta_0(2\theta_1-\theta_0)\right) - \frac{N_{mc}\rho}{N_1 r}\left(m - n\frac{\rho}{1-\rho}\right)\right] \quad (18)$$

$$\beta\mu^{tot} = \beta\mu^{conf}_{QLF} + \beta\mu_{mc} = r\ln\left[1+\left(\frac{q}{r}-1\right)\rho\right] - r\ln(1-\rho) + \ln\left(\frac{\theta_1}{q}\right) + \frac{z\beta}{2}\varepsilon q\left[2\theta_1 - \theta_1^2 + \frac{\beta\varepsilon\theta_0\theta_1}{2}(2\theta_1-\theta_0)\right] + \frac{N_{mc}}{N_1} + 2\ln\left(1-\frac{N_{mc}}{N_1}\right) \quad (19)$$

RESULTS AND DISCUSSION

For pure fluids, a description of the present model requires three classical parameters: cell volume (V_H), segment number (r) and pair interaction energy (ε). Besides these parameters, three others, m, n and χ, are also required to describe the clustering effect, therefore establishing six adjustable parameters for the present model. Although these parameters are empirically defined, we will later discuss how their value and true physical behavior are connected. Model parameters were obtained by adopting a specific regression technique called global regression [32] in which parameters are simultaneously regressed by fitting the model to critical points, supercritical PVT data, saturated vapor pressure and liquid density over a wide temperature range. The objective function for the regression is defined as the sum of average absolute relative deviation (AARD) of the experimental data as follows,

$$F = \frac{100}{NP_1}\sum_{i=1}^{NP_1}\left(\left|\frac{P_i^{exp}-P_i^{cal}}{P_i^{exp}}\right| + \left|\frac{\rho_i^{exp}-\rho_i^{cal}}{\rho_i^{exp}}\right|\right) + \frac{100}{NP_2}\sum_{j=1}^{NP_2}\left|\frac{\rho_j^{sup,exp}-\rho_j^{sup,cal}}{\rho_j^{sup,exp}}\right| + \frac{100}{3}\left(\left|\frac{P_c^{exp}-P_c^{cal}}{P_c^{exp}}\right| + \left|\frac{P_c^{exp}-P_c^{cal}}{P_c^{exp}}\right| + \left|\frac{P_c^{exp}-P_c^{cal}}{P_c^{exp}}\right|\right) \quad (20)$$

where NP_1 and NP_2 represent experimental data for saturated properties and supercritical PVT data, respectively, and superscripts L,

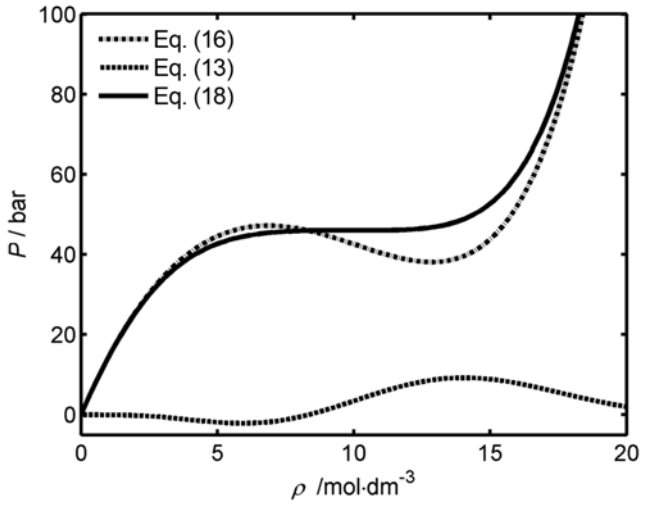

Fig. 4. Calculated pressure contributions for methane at 190.56 K.

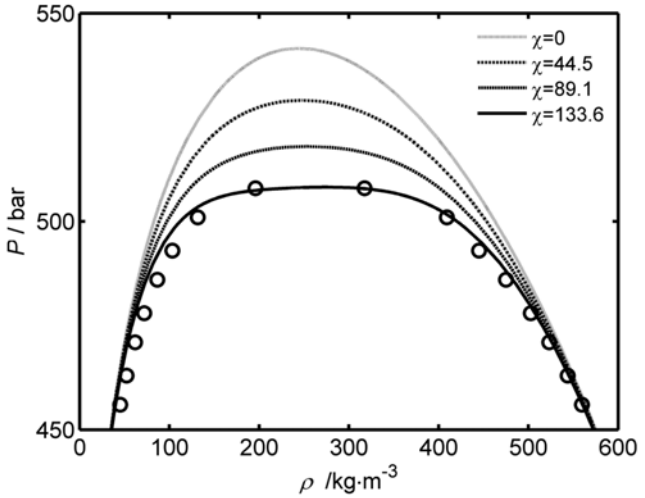

Fig. 5. Calculated T-ρ coexistence curves of acetone by the present model at different magnitudes of the model parameter, χ.

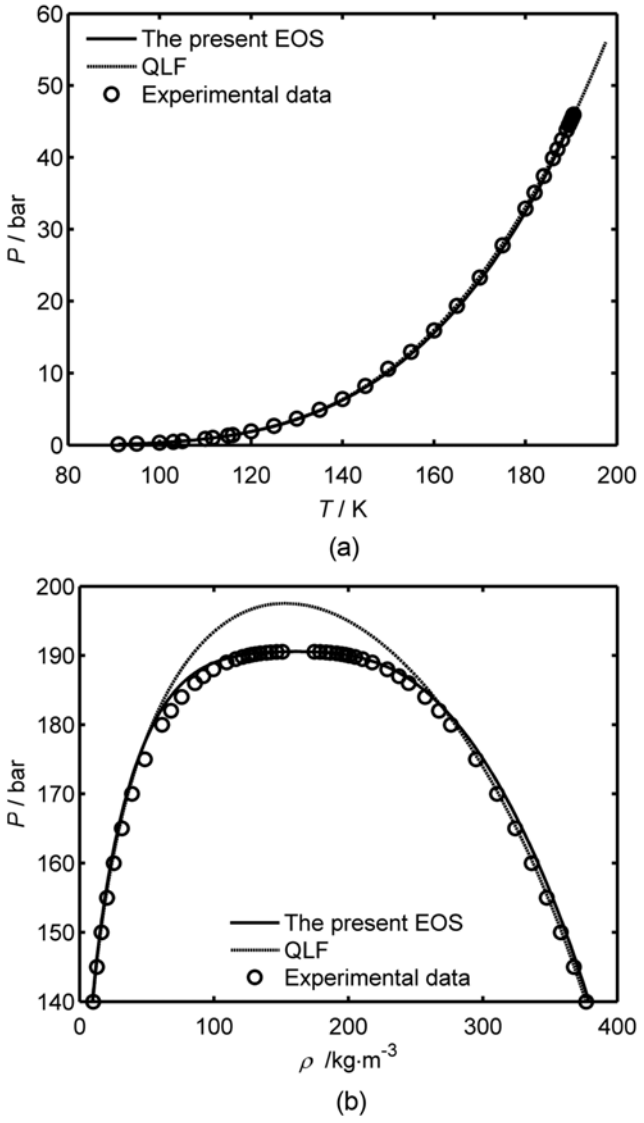

Fig. 6. (a) Correlated vapor pressure against temperature for methane with the basic QLF EOS and the present model. (b) Temperature against correlated saturated density for methane with the basic QLF EOS and the present model.

exp and cal stand for liquid phase, experimental data and calculated data, respectively. Table 1 presents the optimized parameters for the present models, the AARD (%) of vapor pressure and the saturated liquid density for 43 components. Most components have an AARD less than 3.6% and 2.4% for saturated vapor pressure and saturated liquid density, respectively. The average AARD for all components is 2.1% for saturated vapor pressure and 1.2% for saturated liquid density. In Table 2, we list the deviation of correlated critical points from the experimental data [33]. The present model reproduces P_c within 0.73%, T_c within 0.18% and ρ_c within 0.14% of AARD. These small deviations indicate the constraints generated by the critical point do not impair the accuracy of the VLE calculation.

We further investigate how the proposed contribution improves volumetric behavior near the critical region. Fig. 4 shows the calculated isotherm for methane at the experimental critical temperature. The dotted, dash-dotted and solid lines represent proposed contribution of Eq. (13), basic QLF EOS of Eq. (16) and combined model of Eq. (18), respectively. The proposed contribution was found to have negative value at a density below 133.6 $kg \cdot m^{-3}$ (or 8.34 mol/dm^3) and positive value at a density above 133.6 $kg \cdot m^{-3}$. When combined with basic QLF EOS, this behavior forces the present model to exhibit a wide, flat isotherm around the experimental critical density, 162 $kg \cdot m^{-3}$ (or 10.12 mol/dm^3).

The physical meaning of the model parameter is crucial to understanding characteristics of the model. We found that some physical meaning can be assigned to the empirically introduced parameters. Fig. 5 shows the effect of χ on the T-ρ coexistence curve for acetone. The dotted, dash-dotted, short-dashed and solid lines are calculated coexistence curve at χ=0, 44.5, 89.1 and 133.6, respectively. One might expect the top of the coexistence curve to become flattened as χ increases. This behavior implies that χ is strongly as-

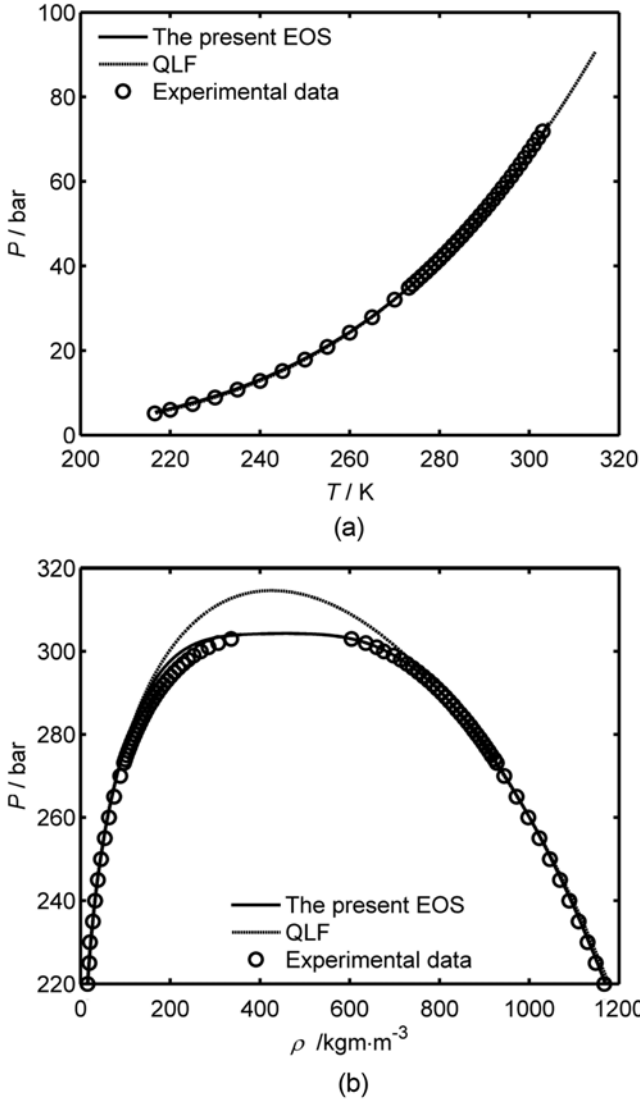

Fig. 7. (a) Correlated vapor pressure against temperature for carbon dioxide with the basic QLF EOS and the present model. (b) Temperature against correlated saturated density for carbon dioxide with the basic QLF EOS and the present model.

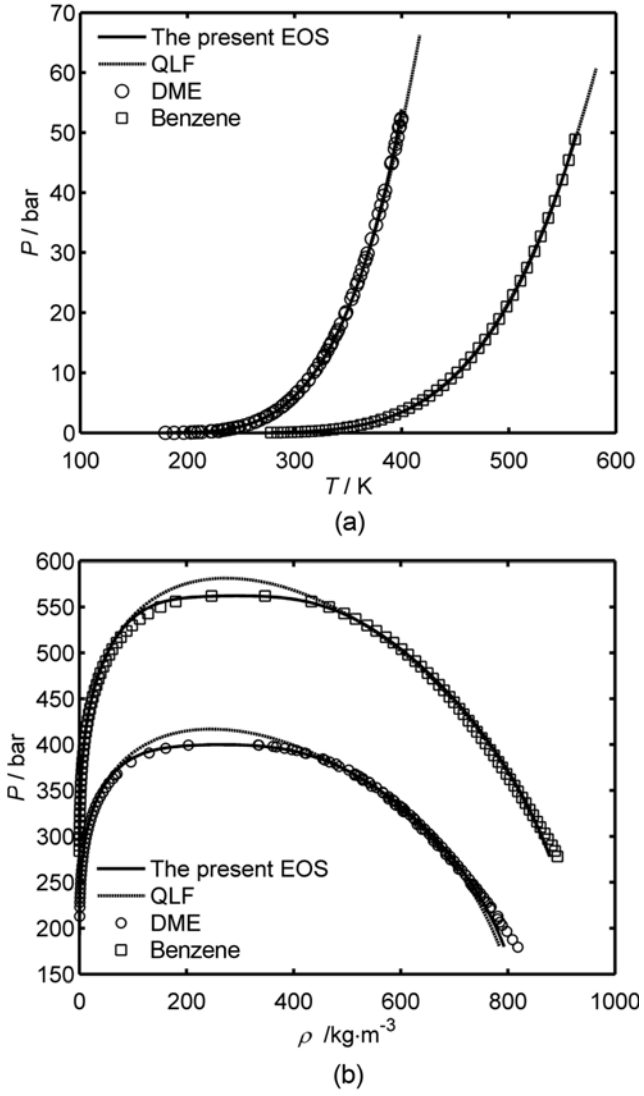

Fig. 8. (a) Correlated vapor pressure against temperature for dimethylether and benzene with the basic QLF EOS and the present model. (b) Temperature against correlated saturated density for dimethylether and benzene with the basic QLF EOS and the present model.

sociated with the strength of the long-range density fluctuation, which can be inferred in Eq. (15). Its role is similar to that of other numbers in renormalization group theory [17].

It is a fundamental attribute for an EOS to accurately correlate volumetric properties such as saturated liquid density and supercritical PVT data. We compared the present model with the basic QLF EOS and represent a few performance indicators in Figs. 6 to 10. For the parameters of the basic QLF, the optimized parameters in the literature [29] were used, but the parameters for carbon dioxide were fitted to the same experimental data used in the present model. Figs. 6 and 7 correlate the results of two models that focus on methane and carbon dioxide, the representatives of the non-polar gases. It is clear that the present model follows the basic QLF EOS in the mean-field region while reproducing the flatness located at the top of the coexistence curve. The basic QLF EOS is found to over-predict the critical temperature and pressure. Figs. 8 and 9 show

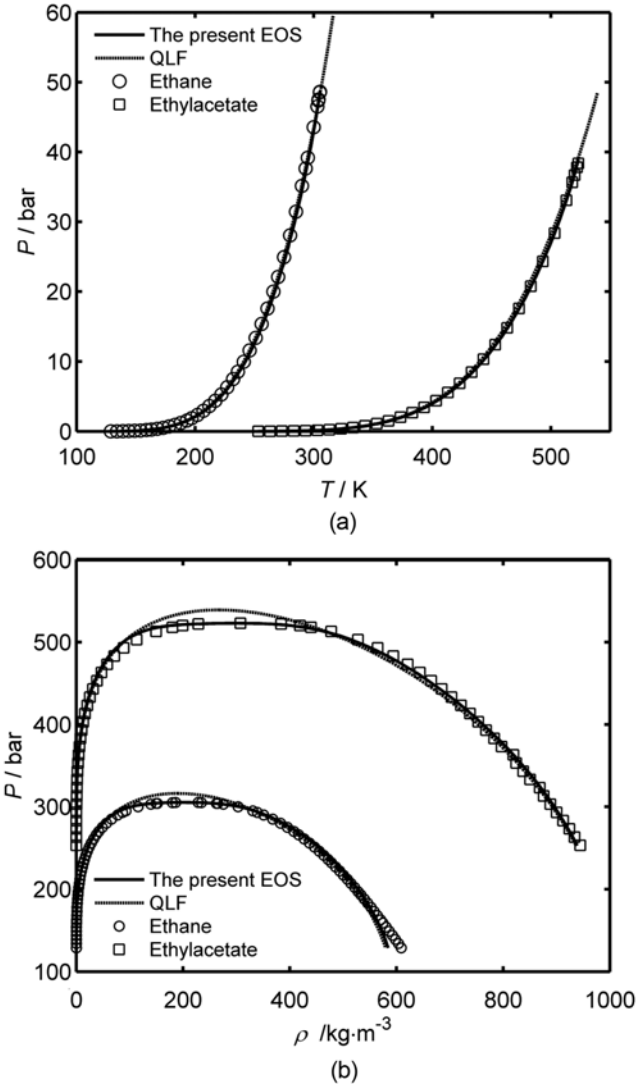

Fig. 9. (a) Correlated vapor pressure against temperature for ethane and ethylacetate with the basic QLF EOS and the present model. (b) Temperature against correlated saturated density for ethane and ethylacetate and benzene with the basic QLF EOS and the present model.

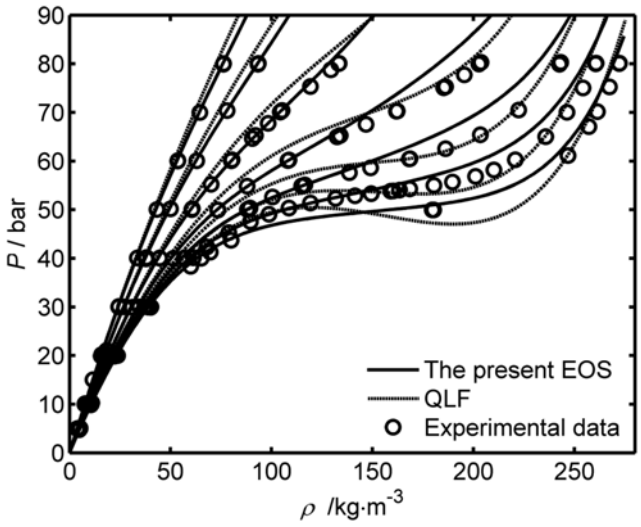

Fig. 10. Correlated supercritical isotherms of methane with the basic QLF EOS (dotted lines) and the present model.

that the saturated vapor pressures and saturated density curves of DME, benzene, ethane and ethyl acetate belong to different groups. The present model satisfactorily reproduces the flatness of the top of the coexistence curve and corresponds well to the experimental data. Fig. 10 shows the calculated supercritical isotherm for methane. The results are in good agreement with experimental data [34]. AARD for the supercritical PVT data of methane is 2.79%.

CONCLUSIONS

We present a new formulation of long-range density fluctuation in terms of molecular clustering. The molecular clustering effect is modeled by extending Veytsman statistics and incorporated into the basic QLF EOS. Adding a fluctuation contribution to the EOS such as SAFT and QLF EOS was found to require a shift in density where the fluctuation contribution is maximized. The combined model was found to reproduce the flatness located at the top of coexistence curve as well as the critical isotherm of methane.

Although the proposed contribution is derived from a framework based upon lattice fluid, it is applicable to other classical equations of state that overpredict the critical temperature and pressure. This is mainly because the proposed contribution provides a negative and positive pressure correction to the vapor-like and liquid-like regions, respectively. Therefore, the proposed contribution can be applicable to the SAFT framework if the relation between the SAFT and lattice fluid variables is properly defined. A combined contribution based on a different theory was already proposed and tested [35, 36]. For example, Gupta and Johnston incorporated original Veytsman statistics into the SAFT and showed a good correlation result with experimental saturated properties as well as molecular simulation.

When compared with other analytic fluctuation terms, the proposed contribution is distinctly different in nature. From the viewpoint of a pressure correction, the present approach gives a negative and positive pressure correction to the vapor-like and liquid-like regions, respectively. Some terms [6,7] show a opposite sign in pressure correction as compared with that of present model or have a

positive sign over the whole density region because their classical EOS does not overpredict the critical temperature and pressure. Thus, using these fluctuation terms, it is difficult to improve the EOS that overpredicts the critical temperature and pressure.

Another difference lies in the strategy of obtaining the fluctuation contribution. The present approach yields a fluctuation contribution effect by solving a quadratic equation as a function of density and tem perature. However, other analytic fluctuation terms are expressed as polynomials [7] or as a Gaussian error function [8]. The quadratic equation for describing the fluctuation contribution is found to be employed in recently developed crossover approach [37]. This implies that quadratic equations are effective in representing the fluctuation effect.

ACKNOWLEDGMENT

This work was supported by the BK21 project of Ministry of Knowledge Economy of Korea and funded by the Korean government (MEST) (No. 2009-0078957).

NOMENCLATURE

a : number of acceptor in component
A : helmholtz energy
d : number of donor in component
k : boltzmann constant
m : component-specific constant in Eq. (9)
n : component-specific constant in Eq. (9)
N_1 : number of molecules
N_r : total number of lattice sites
p : probability for clustering formation
P : pressure
P_c : critical pressure
r : segment length of component or size parameter
R : gas constant
S : entropy
T : temperature (in Kelvin)
T_c : critical temperature
V_H : unit cell volume of lattice
U : internal energy

Greek Letters

μ : chemical potential
ρ : reduced density defined as $N_r/(N_0+N_r)$
ρ_c : critical density
ρ_{hc} : closed packed density
ρ_m : molar density
Ω : partition function
Ξ : exact number of ways to distribute clustered pair among donor and acceptor
Ξ_0 : possible number of ways to distribute clustered pair among donor and acceptor
χ : strength of molecular clustering
ε : interaction energy between molecules

Superscript

conf : configurational property
sat : saturated properties

Subscripts

cla : classical contribution
mc : molecular clustering
HB : Hydrogen bonding
QLF : QLF EOS
tot : total contribution

REFERENCES

1. G. Soave, *Chem. Eng. Sci*., **27**, 1197 (1972).
2. D.-Y. Peng and D. B. Robinson, *Ind. Eng. Chem. Fund*., **15**, 59 (1976).
3. S. H. Huang and M. Radosz, *Ind. Eng. Chem. Res*., **29**, 2284 (1990).
4. M. A. Anisimov, A. A. Povodyrev and J. V. Sengers, *Fluid Phase Equilib*., **158-160**, 537 (1999).
5. J. V. Sengers, *International union of pure and applied chemistry*, Commission on Thermodynamics., Equations of state for fluids and fluid mixtures, 1st ed., Elsevier, Amsterdam, New York (2000).
6. G. F. Chou and J. M. Prausnitz, *AlChE J*., **35**, 1487 (1989).
7. T. Kraska and U. K. Deiters, *Int. J. Thermophys*., **15**, 261 (1994).
8. C. J. Kedge and M. A. Trebble, *Fluid Phase Equilib*., **194-197**, 401 (2002).
9. S. B. Kiselev, *Fluid Phase Equilib*., **147**, 7 (1998).
10. J. Jianwen and J. M. Prausnitz, *J. Chem. Phys*., **111**, 5964 (1999).
11. K. G. Wilson, *Physical Review B*, **4**, 3174 (1971).
12. K. G. Wilson, *Physical Review B*, **4**, 3184 (1971).
13. W. S. Liming and A. W. John, *J. Chem. Phys*., **96**, 4559 (1992).
14. A. W. John and Z. Sheng, *J. Chem. Phys*., **103**, 1922 (1995).
15. L. D. Landau, E. M. Lifshitz and L. P. Pitaevskii, *Statistical physics*, 3d rev. and enl. ed., Pergamon Press, Oxford, New York (1980).
16. F. Fornasiero and L. L. A. Bertucco, *AlChE J*., **45**, 906 (1999).
17. J. Mi, C. Zhong and Y.-G. Li, *J. Chen, Chem. Phys*., **305**, 37 (2004).
18. S. B. Kiselev and J. F. Ely, *Ind. Eng. Chem. Res*., **38**, 4993 (1999).
19. M. S. Shin, Y. Lee and H. Kim, *J. Chem. Thermodyn*., **40**, 174 (2008).
20. J. Mi, Y. Tang, C. Zhong and Y. G. Li, *J. Phys. Chem. B*, **109**, 20546 (2005).
21. R. A. Heidemann and J. M. Prausnitz, Proceedings of the National Academy of Sciences, **73**, 1773 (1976).
22. M. S. Wertheim, *J. Stat. Phys*., **35**, 35 (1984).
23. M. S. Wertheim, *J. Stat. Phys*., **35**, 19 (1984).
24. B. A. Veytsman, *J. Phys. Chem*., **94**, 8499 (1990).
25. D. M. Pfund, T. S. Zemanian, J. C. Linehan, J. L. Fulton and C. R. Yonker, *J. Phys. Chem*., **98**, 11846 (1994).
26. S. C. Tucker, *Chem. Rev*., **99**, 391 (1999).
27. S. C. Tucker and M. W. Maddox, *J. Phys. Chem. B*, **102**, 2437 (1998).
28. C. S. Lee, J. W. Kang, J. H. Lee and K.-P. Yoo, *Fluid Phase Equilib*., **265**, 215 (2008).
29. M. S. Shin and H. Kim, *Fluid Phase Equilib*., **246**, 79 (2006).
30. J. M. H. Levelt Sengers, *Fluid Phase Equilib*., **158-160**, 3 (1999).
31. C. Panayiotou and I. C. Sanchez, *J. Phys. Chem*., **95**, 10090 (1991).
32. C. J. Kedge and M. A. Trebble, *Fluid Phase Equilib*., **217**, 257 (2004).
33. R. H. Perry, D. W. Green and J. O. Maloney, *Perry's chemical engi-*

neers' handbook, 7th ed., McGraw-Hill, New York (1997).
34. G. Handel, R. Kleinrahm and W. Wagner, *J. Chem. Thermodyn*., **24**, 685 (1992).
35. S. O. Derawi, M. L. Michelsen, G. M. Kontogeorgis and E. H. Stenby, *Fluid Phase Equilib*., **209**, 163 (2003).
36. R. B. Gupta and K. P. Johnston, *Fluid Phase Equilib*., **99**, 135 (1994).
37. S. B. Kiselev and J. F. Ely, *Chem. Eng. Sci*., **61**, 5107 (2006).
38. N. B. Vargaftik, Y. K. Vinogradov and V. S. Yargin, *Handbook of physical properties of liquids and gases: Pure substances and mixtures*, 3rd augm. and rev. ed., Begell House, New York (1996).
39. R. Kleinrahm and W. Wagner, *J. Chem. Thermodyn*., **18**, 739 (1986).
40. B. D. Smith and R. Srivastava, *Thermodynamic data for pure compounds*, Elsevier, Distributors for the U.S. and Canada, Elsevier Science Pub. Co., Amsterdam, New York, U.S.A. (1986).
41. T. E. Daubert and R. P. Danner, Design Institute for Physical Property Data (U.S.), *Physical and thermodynamic properties of pure chemicals: data compilation*, Hemisphere Pub. Corp., New York (1989).
42. P. Nowak, R. Kleinrahm and W. Wagner, *J. Chem. Thermodyn*., **28**, 1441 (1996).
43. E. C. Ihmels and E. W. Lemmon, *Fluid Phase Equilib*., **260**, 36 (2007).
44. W. Braker and A. L. Mossman, *Matheson Company inc., Matheson gas data book*, 6th ed., Matheson, Lyndhurst, NJ (1980).
45. J. Wu, Z. Liu, J. Pan and X. Zhao, *J. Chem. Eng. Data*, **49**, 32 (2004).
46. J. Wu, Z. Liu, B. Wang and J. Pan, *J. Chem. Eng. Data*, **49**, 704 (2004).